PSFC/RR-99-9

BELINE: a code for calculating the profiles of hydrogen spectral lines emitted from divertor tokamak plasma

L.G. D'yachkov[3], V.G. Novikov[2], A.F. Nikiforov[2]
A. Yu. Pigarov[1], V.S. Vorob'ev[3]

July 1999

[1] Plasma Science and Fusion Center, Massachusetts Institute of Technology, Cambridge, MA 02139, U.S.A.

[3] Institute for High Temperatures, Izorskaya 13/19, Moscow, 127412, Russia

[2] Keldysh Institute of Applied Mathematics, Miusskya pl.4, Moscow, 125047, Russia

BELINE:
a code for calculating the profiles of hydrogen spectral lines emitted from divertor tokamak plasmas

L.G.D'yachkov[1], V.G.Novikov[2], A.F.Nikiforov[2], A.Yu.Pigarov[3], V.S.Vorob'ev[1]

[1] Institute for High Temperatures, Izorskaya 13/19, Moscow, 127412, Russia

[2] Keldysh Institute of Applied Mathematics, Miusskya pl.4, Moscow, 125047, Russia

[3] Plasma Science and Fusion Center, Massachusetts Institute of Technology, Cambridge, MA 02139, USA

Abstract

A direct method for calculation of hydrogenic spectral line profiles in the external magnetic field is developed. The corresponding code BELINE can calculate any line profile for emitting hydrogen or deuterium plasmas in a wide range of tokamak divertor conditions. The code is based on the solution of the quantum-mechanical problem associated with emitting hydrogen atom placed in crossing external magnetic and quasi-static (ion) electric fields. In the fields a $\bar{n}-n$ hydrogenic line splits into $n^2\bar{n}^2$ components, for each component the interaction with free electrons and atom motion (Doppler effect) are taken into account and the result is averaged over electrical field distribution function. One case of temperature and density takes approximately several minutes running. The results for 3-2 and 8-2 Balmer lines of deuterium plasma are presented in dependency on electron density.

§1. Introduction

Previously in report [1], when solving a radiative transfer problem, we used simplest spectral line shapes without considering influence of external magnetic field on the line profile. However, the value of magnetic field in the edge plasma is strong enough (about 6-12 T) and has a significant action on spectral line shapes and hence on radiative transfer as a whole.

A special code named as BELINE was constructed to calculate spectral line shapes in the presence of external magnetic field including averaging over internal plasma electric microfield. To produce this result we solve quantum-mechanical problem associated with a radiating atom in crossing electric and magnetic fields taking into account Doppler effect and averaging over electric field distribution function. The fact that the spectral line shape depends on the direction of observation adds complexity and increases the computing time. A special procedure using matrix representation was developed to reduce the computing time. The calculations for deuterium Balmer spectral lines 3-2 and 8-2 were carried out. Particular emphasis has been made on the 8-2 line, playing important role in the divertor plasma diagnostics. For the 8-2 line we present the profiles calculated without and with magnetic field for different directions of observation. The electron density dependencies of the line width obtained using different approximations of electron broadening are given also.

§2. Hydrogenic spectral line profiles

The strong external magnetic field and internal electric plasma microfield generated by fluctuations of ions and electrons, give rise to a considerable influence on the shape of spectral lines. Usually ion microfield can be considered in the quasi-static approximation while electron microfield – in the impact approximation [2]. When a hydrogenic atom is subjected to both electric and magnetic fields, degeneration is taken away and each line splits into $n^2\bar{n}^2$ components where n and $\bar{n}$ are the principal quantum numbers of the lower and upper transition states respectively. We consider the case when the fields are strong enough and the spin-orbit interaction can be disregarded. The splitting structure is more complex than structute under action by one of the fields. The shift and intensity of a component depend on the

values of magnetic field $\mathbf{B}$ and quasi-static electric field $\mathbf{E}$ and the angle between vectors $\mathbf{B}$ and $\mathbf{E}$. Besides, the intensity (but not the shift) depends on the angles between radiative direction $\mathbf{K}$ and vectors $\mathbf{B}$ and $\mathbf{E}$ (unit vector $\mathbf{K}$ is defined by $\mathbf{K} = \mathbf{k}/|\mathbf{k}|$ where $\mathbf{k}$ is the wave vector). The profile of each component is determined by the Doppler effect and electron collisions.

1. Splitting structure

We can present the total profile of the spectral line for a $\bar{n} \to n$ transition as a sum of different component profiles taking into account the averaging over the value and direction of the quasi-static ion microfield

$$\Phi_{\bar{n}n}(\omega) = \frac{1}{4\pi} \int dO_E \int_0^\infty P(E) \sum_{\bar{\nu}\nu} G_\nu^{\bar{\nu}} \cdot \phi_\nu^{\bar{\nu}}(\omega) dE \tag{1}$$

where $P(E)$ is the quasi-static electric microfield distribution function, $\phi_\nu^{\bar{\nu}}(\omega)$ and $G_\nu^{\bar{\nu}}$ are the profile and intensity of the $\bar{\nu} \to \nu$ component respectively. Here $\bar{\nu}$ and ν denote complete sets of the quantum numbers determining initial and final atomic states in the fixed magnetic $\mathbf{B}$ and electric $\mathbf{E}$ fields.

We calculate the profile of a component $\phi_\nu^{\bar{\nu}}(\omega)$ taking into account the Doppler effect and electron collisions as a convolution of corresponding profiles

$$\phi_\nu^{\bar{\nu}}(\omega) = \frac{1}{\sqrt{\pi} D_{\nu\bar{\nu}}} \int \psi_\nu^{\bar{\nu}}(\omega - \omega_{\nu\bar{\nu}} - s) e^{-(s/D_{\nu\bar{\nu}})^2} \, ds \tag{2}$$

where $\omega_{\bar{\nu}\nu}$ is the center of the $\nu\bar{\nu}$ component, $D_{\nu\bar{\nu}} = (\omega_{\nu\bar{\nu}}/c)(2T_a/M)^{1/2}$ is the Doppler broadening parameter, c is the velocity of light, T_a is the atomic temperature and M is the atom mass. For the electron profile $\psi_\nu^{\bar{\nu}}$ we use different approximations considered in following subsection.

Relative intensities of the $\bar{\nu} \to \nu$ components are estimated in the dipole approximation

$$G_\nu^{\bar{\nu}} = \frac{|\mathbf{e}_\rho \langle \nu | \mathbf{r} | \bar{\nu} \rangle|^2}{\sum\limits_{\nu\bar{\nu}} |\mathbf{e}_\rho \langle \nu | \mathbf{r} | \bar{\nu} \rangle|^2} \tag{3}$$

where $\mathbf{e}_\rho$ is the unit polarization vector. For nonpolarized radiation (in atomic units)

$$G_\nu^{\bar\nu} = \frac{\omega_{n\bar n}}{n^2 f_{n\bar n}} \sum_{\rho=1,2} |\mathbf{e}_\rho \langle \nu|\mathbf{r}|\bar\nu\rangle|^2 \qquad (4)$$

where $f_{n\bar n}$ is the total oscillator strength of the $\bar n$–n transition.

Let us assume that the fields are sufficiently strong, so that the spin-orbit interaction can be disregarded: $E \gg \dfrac{\alpha^2}{6n^4} \simeq \dfrac{5\cdot 10^4}{n^4}$ V/cm, $B \gg \dfrac{\alpha}{2n^3} \simeq \dfrac{6}{n^3}$ T where $\alpha = 1/137$ is the fine structure constant. On the other hand, the fields must be lower than atomic ones for radiating states, so the typical value of the line splitting is small with respect to the line spacing and we can regard the line $\bar n - n$ as isolated. It has been shown in the framework of the old Bohr theory [3] that simultaneous effect of magnetic and electric fields on the $n\ell$ electron orbit can be described in the first approximation as an uniform and independent precession of vectors $\frac{3}{2}n\mathbf{L} \pm \mathbf{r}_a$ ($\mathbf{L}$ is the angular momentum and $\mathbf{r}_a$ is the radius-vector of the electron averaged over the orbital motion) with angular velocities

$$\mathbf{\Omega}_{1,2} = \frac{\alpha}{2}\,\mathbf{B} \mp \frac{3}{2}\,n\mathbf{E}.$$

Correction to the electron energy has been obtained in the same approximation [3]. Quantum-mechanical consideration gives the same result in the first order of the perturbation theory [4]. We can write the Hamiltonian as a sum

$$\mathcal{H} = \mathcal{H}_0 + \mathcal{H}_1$$

of the unperturbed Hamiltonian

$$\mathcal{H}_0 = -\frac{1}{2}\Delta - \frac{1}{r}$$

and perturbation

$$\mathcal{H}_1 = \frac{\alpha}{2}\mathbf{BL} + \mathbf{Er}.$$

The last can be presented in the form

$$\mathcal{H}_1 = \frac{\alpha}{2}\mathbf{BL} - \frac{3}{2}n\mathbf{EA} = \mathbf{\Omega}_1\mathbf{I}_1 + \mathbf{\Omega}_2\mathbf{I}_2$$

where $\mathbf{I}_{1,2} = \frac{1}{2}(\mathbf{L} \pm \mathbf{A})$, $\mathbf{A}$ is the Runge–Lenz vector for which in this case we have $\mathbf{A} = 2\mathbf{r}/(3n)$ [4].

Operators $\mathbf{I}_{1,2}$ are commutative with $\mathcal{H}_0$ and satisfy the usual relations of the ordinary angular momentum operators. So, $I_1^2 = I_2^2 = j(j+1)$, where j is determined by whole number of states $(2j+1)^2 = n^2$ and hence $j = (n-1)/2$. Projection n' of $\mathbf{I}_1$ to the direction $\mathbf{\Omega}_1$ and projection n'' of $\mathbf{I}_2$ to the direction $\mathbf{\Omega}_2$ may be any of $2j+1$ integer or half-integer values $-j,\ -j+1,\ \ldots,\ j-1,\ j$.

In first order of the perturbation theory

$$\varepsilon_{nn'n''m_s} = -\frac{1}{2n^2} + \Omega_1 n' + \Omega_2 n'' + \alpha B m_s \tag{5}$$

where $m_s = \pm\frac{1}{2}$ is the spin projection on the magnetic field direction.

We can write eigenstate $\psi_{n'n''}$ as a linear combination of the Stark eigenstates corresponding to separation of variables in parabolic coordinates with z axis along the electric field $\mathbf{E}$

$$\psi_{n'n''} = \sum_{i_1=-j}^{j} \sum_{i_2=-j}^{j} d^j_{n'i_1}(\alpha_1) d^j_{n''i_2}(\alpha_2)\, \psi_{i_1 i_2} \tag{6}$$

where $d^j_{kk'}(\alpha) = D^j_{kk'}(0, \alpha, 0)$ is the Wigner function [5] corresponding to the turn about the z axis of an angle α and $\psi_{i_1 i_2} \equiv \psi_{nn_1n_2m}$ is the wave function in parabolic coordinates. In our case it is convenient to mark this function with the quantum numbers i_1 and i_2 which are the projections of $\mathbf{I}_1$ and $\mathbf{I}_2$ to the z axis respectively and their relations with ordinary parabolic n_1, n_2 and magnetic m quantum numbers are

$$m = i_1 + i_2,$$

$$n_1 = \frac{1}{2}\,(n - |m| - 1 + i_2 - i_1),$$

$$n_2 = \frac{1}{2}\,(n - |m| - 1 + i_1 - i_2).$$

Angles α_1 and α_2 are those between $\mathbf{E}$ and vectors $\mathbf{\Omega_1}$ and $\mathbf{\Omega_2}$ respectively, i.e.

$$\cos\alpha_{1,2} = \frac{\frac{\alpha}{2} B \cos\,\vartheta \mp \frac{3}{2} nF}{\Omega_{1,2}}$$

where ϑ is the angle between $\mathbf{B}$ and $\mathbf{E}$.

The shift of a $\bar{\nu} \to \nu$ component ($\nu \equiv nn'n''$) follows from (5) disregarding the spin-orbit interaction

$$\omega_{\nu\bar{\nu}} - \omega_{n\bar{n}} = \bar{\Omega}_1\bar{n}' + \bar{\Omega}_2\bar{n}'' - \Omega_1 n' - \Omega_2 n''$$

where $\omega_{n\bar{n}}$ is the shift of the unperturbed line $\bar{n} - n$.

Dipole matrix elements in (3) and (4) between states (6) can be presented in the form of linear combination of the matrix elements between states $\psi_{i_1 i_2}$. Let us $e_{\rho x},\ e_{\rho y},\ e_{\rho z}$ are the Cartesian coordinates of the unit polarization vector $\mathbf{e}_\rho$ in the coordinate system with z axis along $\mathbf{E}$ and x axis lying in the plane defined by the vectors $\mathbf{B}$ and $\mathbf{E}$. Then

$$\mathbf{e}_\rho\langle\bar{\nu}|\mathbf{r}|\nu\rangle = \sum_{a=x,y,z} e_{\rho a}\langle\bar{\nu}|a|\nu\rangle,$$

$$\langle\bar{\nu}|a|\nu\rangle \equiv \langle\bar{n}\bar{n}'\bar{n}''\,|a|\,nn'n''\rangle$$

$$= \sum_{i_1=-j}^{j}\sum_{i_2=-j}^{j}\sum_{\bar{i}_1=-\bar{j}}^{\bar{j}}\sum_{\bar{i}_2=-\bar{j}}^{\bar{j}} d^j_{n'i_1}(\alpha_1)\, d^j_{n''i_2}(\alpha_2) d^{\bar{j}}_{\bar{n}'\bar{i}_1}(\bar{\alpha}_1)\, d^{\bar{j}}_{\bar{n}''\bar{i}_2}(\bar{\alpha}_2)\langle\bar{n}\bar{n}_1\bar{n}_2\bar{m}|a|nn_1n_2m\rangle \tag{7}$$

where matrix elements $\langle\bar{n}\bar{n}_1\bar{n}_2\bar{m}|a|nn_1n_2m\rangle$ are calculated from the Gordon formulas [6].

In the case of nonpolarized radiation we put $\mathbf{e}_1$ being normal to the plane of the vectors $\mathbf{K}$ and $\mathbf{B}$, while $\mathbf{e}_2$ lying in this plane and normal to $\mathbf{K}$. For averaging over $\mathbf{E}$ directions in (1), we introduce the spherical coordinate system with z axis along $\mathbf{B}$. Denote by $\widetilde{\vartheta}$ the angle between $\mathbf{B}$ and $\mathbf{K}$ and by φ the angle between projections of $\mathbf{K}$ and $\mathbf{E}$ into the plane normal to $\mathbf{B}$. Then

$$e_{1x} = \cos\vartheta\sin\varphi, \quad e_{1y} = \cos\varphi, \quad e_{1z} = \sin\vartheta\sin\varphi;$$

$$e_{2x} = -\cos\widetilde{\vartheta}\cos\vartheta\cos\varphi - \sin\widetilde{\vartheta}\sin\vartheta, \quad e_{2y} = \cos\widetilde{\vartheta}\sin\varphi,$$

$$e_{2z} = -\cos\widetilde{\vartheta}\sin\vartheta\cos\varphi + \sin\widetilde{\vartheta}\cos\vartheta.$$

Following calculations depend on the approximation using for the electron broadening evaluation. If the profiles of $\bar{\nu}$–ν components do not depend on

the angle φ , we can make integration over φ in (1) in analytical manner and get

$$\Phi_{\bar{n}n}(\omega) = \frac{\omega_{n\bar{n}}}{4n^2 f_{n\bar{n}}} \int_0^\infty dE P(E) \sum_{\nu\bar{\nu}} \int_0^\pi d\vartheta \sin\vartheta \, \phi_{\nu\bar{\nu}}(\omega)$$

$$\cdot \left\{ 2\sin^2\widetilde{\vartheta}(x_\nu^{\bar{\nu}}\sin\vartheta - z_\nu^{\bar{\nu}}\cos\vartheta)^2 + (1+\cos^2\widetilde{\vartheta}) \left[(x_\nu^{\bar{\nu}}\cos\vartheta + z_\nu^{\bar{\nu}}\sin\vartheta)^2 + (y_\nu^{\bar{\nu}})^2 \right] \right\}$$

where matrix elements $a_\nu^{\bar{\nu}} \equiv \langle \nu|a|\bar{\nu}\rangle$ $(a = x, y, z)$ are defined by equation (7).

The Wigner function $d^j_{kk'}(\alpha)$ in (6) and (7) can be expressed in the terms of the Jacobi polynomials [5]:

$$d^j_{kk'}(\alpha) = \xi_{kk'} \left[\frac{s!(s+\mu+\nu)!}{(s+\mu)!(s+\nu)!} \right]^{1/2} \left(\sin\frac{\alpha}{2} \right)^\mu \left(\cos\frac{\alpha}{2} \right)^\nu P_s^{(\mu,\nu)}(\cos\alpha)$$

where $\mu = |k-k'|$, $\nu = |k+k'|$, $s = j - \frac{1}{2}(\mu+\nu)$, $\xi_{kk'} = 1$ if $k' \geq k$ and $\xi_{kk'} = (-1)^{k'-k}$ if $k' < k$. It is convenient to calculate the Jacobi polynomials by means of the recurrence relations [7].

2. Electron broadening

For the calculation of the $\bar{\nu}$–ν component profiles due to electron collisions, we use three different approximations corresponding to different accuracy related with spectrum details.

1) First, we consider the simplest approximation which gives the same profile for all the $\bar{\nu}$–ν components for a given $\bar{n}$–n line. According to the impact approximation, the electron profile is assumed as the Lorentz one

$$\psi_\xi(u) = \frac{\gamma/2\pi}{u^2 + \gamma^2/4} \tag{8}$$

where ξ denotes the component $\bar{\nu} \to \nu$ $(\bar{n}\bar{n}'\bar{n}'' \to nn'n'')$ in the spectral line $\bar{n} \to n$ and $u = \omega - \omega_{\nu\bar{\nu}}$ is the distance from the component center. The width γ is estimated by the equation [8, 9]

$$\gamma = \frac{32}{3}\frac{n_e}{v_e}\left(\ln\frac{R_m}{R_w} + 0.215 \right)\left(n^4 + n'^4 \right) \tag{9}$$

where v_e is the mean velocity of the electrons, R_W is the Weisskopf radius and R_m is the upper limit for the impact parameter. For simplicity, we substitute the Debye radius for R_m, although in this case in the far line wings the condition of applicability of the impact approximation will be violated.

Equation (9) gives a mean value over all component widths, although more correct approximation shows considerable difference between these widths. However, the use of this equation is justified by the fact that the line broadening is determined also by ion and Doppler ones. Only for central components the electron broadening can be more important, while for outlying components the ion broadening should apparently be dominant.

2) For more accurate calculations we use the same profile (8), while the width is evaluated as

$$\gamma = \gamma_n^{(e)} + \gamma_{\bar{n}}^{(e)} + \gamma_{n\bar{n}}^{(u)}.$$

Here

$$\gamma_n^{(e)} = \frac{1}{n^2} \sum_{\ell m n' \ell' m'} \gamma^{(e)}_{n\ell m, n'\ell' m'}, \quad \gamma_{n\bar{n}}^{(u)} = \frac{1}{n^2 \bar{n}^2} \sum_{\ell m \ell' m'} \gamma^{(u)}_{n\ell m, \bar{n}\ell' m'} \tag{10}$$

where $\gamma^{(e)}_{n\ell m, n'\ell' m'}$ is the probability of electron transition in unit time from state $n\ell m$ to state $n'\ell' m'$ due to interaction with free electrons, which is possible to be written as [10, 11]:

$$\gamma^{(e)}_{n\ell m, n'\ell' m'} = 2\pi \iint n(\varepsilon)\,[1 - n(\varepsilon')]\, d\varepsilon d\varepsilon' \delta(\varepsilon_{n\ell m} - \varepsilon_{n'\ell' m'} + \varepsilon - \varepsilon') \times$$
$$\times \sum_{\bar{\ell}\bar{m}\bar{\ell}'\bar{m}'} \left| \iint \psi^*_{n\ell m}(\mathbf{r}) \psi^*_{\varepsilon\bar{\ell}\bar{m}}(\mathbf{r}\,') \frac{1}{|\mathbf{r} - \mathbf{r}\,'|} \psi_{n'\ell' m'}(\mathbf{r}) \psi_{\varepsilon'\bar{\ell}'\bar{m}'}(\mathbf{r}\,') d\mathbf{r} d\mathbf{r}\,' \right|^2 . \tag{11}$$

Here $\psi_{n\ell m}(\mathbf{r}) = \frac{1}{r} R_{n\ell}(r) Y_{\ell m}(\vartheta, \varphi)$ and $\psi_{\varepsilon\ell m}(\mathbf{r}) = \frac{1}{r} R_{\varepsilon\ell}(r) Y_{\ell m}(\vartheta, \varphi)$ are the wave functions of bound and free electrons, $n(\varepsilon)$ is the free electron distribution function. The universal broadening [10, 11]

$$\gamma^{(u)}_{n\ell m, n'\ell' m'} = 2\pi \iint n(\varepsilon)\,[1 - n(\varepsilon')]\, d\varepsilon d\varepsilon' \delta(\varepsilon - \varepsilon') \times$$
$$\times \sum_{\bar{\ell}\bar{m}\bar{\ell}'\bar{m}'} \left| \iint \left[|\psi_{n'\ell' m'}(\mathbf{r})|^2 - |\psi_{n\ell m}(\mathbf{r})|^2 \right] \frac{\psi_{\varepsilon\bar{\ell}\bar{m}}(\mathbf{r}\,') \psi_{\varepsilon'\bar{\ell}'\bar{m}'}(\mathbf{r}\,')}{|\mathbf{r} - \mathbf{r}\,'|} d\mathbf{r} d\mathbf{r}\,' \right|^2 . \tag{12}$$

After integrating over angles in (11) and (12), we obtain the following expressions

$$\gamma_n^{(e)} = \frac{1}{n^2} \sum_{\ell n' \ell'} \sum_{s=0}^{\infty} \frac{C^{(s)}_{\ell\ell'}}{2s+1} \gamma^{(s)}_{n\ell, n'\ell'},$$

$$\gamma^{(u)}_{n,\bar{n}} = \frac{1}{n^2\bar{n}^2}\sum_{\ell\ell'}\left[\tilde{\gamma}^{(0)}_{n\ell,\bar{n}\ell'} + \sum_{s=2}^{\infty}\frac{1}{(2s+1)^2}\left(\frac{C^{(s)}_{\ell'\ell'}}{2\ell'+1}\gamma^{(s)}_{\bar{n}\ell',\bar{n}\ell'} + \frac{C^{(s)}_{\ell\ell}}{2\ell+1}\gamma^{(s)}_{n\ell,n\ell}\right)\right]$$

where

$$C^{(s)}_{\ell\ell'} = (2\ell'+1)\begin{pmatrix}\ell & \ell' & s\\ 0 & 0 & 0\end{pmatrix}^2,$$

$$\gamma^{(s)}_{n\ell,n'\ell'} = 4\pi\sum_{\bar{\ell},\bar{\ell}'}(2\bar{\ell}+1)C^{(s)}_{\bar{\ell}\bar{\ell}'}\int n(\varepsilon)\left[1-n(\varepsilon)\right]\left[R^{(s)}_{n'\ ell\ell'n'\ell',\varepsilon\bar{\ell}\varepsilon\bar{\ell}'}R^{(s)}_{n\ell n\ell,\varepsilon\bar{\ell}\varepsilon\bar{\ell}'}\right]d\varepsilon, \tag{13}$$

$$\tilde{\gamma}^{(0)}_{n\ell,n'\ell'} = 4\pi\sum_{\bar{\ell}}(2\bar{\ell}+1)\int n(\varepsilon)\left[1-n(\varepsilon)\right]\left[R^{(0)}_{n'\ell'n'\ell',\varepsilon\bar{\ell}\varepsilon\bar{\ell}} - R^{(0)}_{n\ell n\ell,\varepsilon\bar{\ell}\varepsilon\bar{\ell}}\right]^2 d\varepsilon, \tag{14}$$

$$R^{(s)}_{n\ell n'\ell',\varepsilon\bar{\ell}\varepsilon'\bar{\ell}'} = \iint R_{n\ell}(r_1)R_{\varepsilon\bar{\ell}}(r_2)\frac{r^s_<}{r^{s+1}_>}R_{n'\ell'}(r_1)R_{\varepsilon'\bar{\ell}'}(r_2)dr_1dr_2. \tag{15}$$

Here $r_<$ and $r_>$ are respectively smaller and larger of r_1 and r_2. When calculating integrals $R^{(s)}_{n\ell n'\ell',\varepsilon\bar{\ell}\varepsilon'\bar{\ell}'}$ the semiclassical approximation is used for functions of continuum.

3) For more detailed consideration we use the approximation similar to that presented by Seaton [12] for the case of Stark effect. It is based on the Bethe-Born approximation for the interaction between radiating atom and perturbing electrons, cut-off angular momentum and use of a simple analytical profile. The electron profile is approximated by

$$\psi_\xi(u) = \frac{\gamma_\xi(u)/2\pi}{u^2 + g^2_\xi(u)/4}. \tag{16}$$

Profile (16) is symmetrical, so we put $u > 0$. Functions $\gamma_\xi(u)$, $g_\xi(u)$ are defined by [12]

$$\gamma_\xi(u) = \sqrt{2\pi/T_e}n_eQ_\xi w(u), \tag{17}$$

$$g_\xi(u) = \sqrt{2\pi/T_e}n_eQ_\xi u\int_u^\infty\frac{w(u')}{u'^2}du'. \tag{18}$$

Here T_e is the electron temperature, $w(u)$ depends only on the principal quantum numbers and it is the same for all components, while a factor Q_ξ

does not depend on u, but is defined by all the quantum numbers of initial and final states. In the case under consideration we can take the function $w(u)$ from [12] without any alteration, while the factor Q_ξ should be modified.

Diagonal matrix γ approximates the electron interaction matrix $\mathbf{\Gamma}$ in such a manner that

$$\mathbf{D}^+\gamma\mathbf{D} = \mathbf{D}^+\mathbf{\Gamma}\mathbf{D}$$

where $\mathbf{D}$ is the column matrix of transition probability amplitudes D_ξ, $|D_\xi|^2 = G^p_\nu$. Therefore we can present the factor Q_ξ as a product

$$Q_\xi = bG_{\xi\xi}$$

where $G_{\xi\xi}$ is the diagonal matrix element of matrix $\mathbf{G}$ related with $\mathbf{\Gamma}$ by equation similar to (17) and

$$b = \frac{\sum\limits_{\xi\xi'} D^*_\xi G_{\xi\xi'} D_{\xi'}}{\sum\limits_{\xi} |D_\xi|^2 G_{\xi\xi}}. \tag{19}$$

Seaton [12] gives the corresponding matrix $\mathbf{G}_L$ in the spherical coordinate $n\ell m$ presentation and shows a way how to transform it to the Stark presentation (nn_1n_2m). In our case we should make the transformation into the $nn'n''$ presentation for accounting Stark and Zeeman effects (Stark–Zeeman presentation). This transformation is made by means of the matrix $\mathbf{Y}$:

$$\mathbf{G}{=}\mathbf{Y}\mathbf{G}_L\mathbf{Y}^+$$

where

$$Y_{\xi s} = \langle n\ell m|nn'n''\rangle\langle\bar{n}\bar{\ell}\bar{m}|\bar{n}\bar{n}'\bar{n}''\rangle.$$

Here, by analogy with ξ denoting the transition $\bar{n}\bar{n}'\bar{n}'' \to nn'n''$ between Stark–Zeeman states, s denotes the transition $\bar{n}\bar{\ell}\bar{m} \to n\ell m$.

Taking into account equation (6) and results by Hughes [13], we can write

$$\langle n\ell m|nn'n''\rangle = \sum_{i_1=-j}^{j} (-1)^{j-i_2} d^j_{n'i_1}(\alpha_1)\, d^j_{n''i_2}(\alpha_2) C(j,j,\ell;i_1,i_2,m)$$

where $i_2 = m - i_1$ and $C(a,b,c;\alpha,\beta,\gamma)$ is the Clebsh–Gordan coefficient.

The numerator in (19) can be calculated in any presentation, in particular, in the $n\ell m$ presentation, while the denominator should be calculated in the $nn'n''$ presentation. In this case the dependence of the factor b on the angles ϑ and φ makes analytical integration over φ in (1) impossible.

§3. Results

We have performed calculations for typical conditions in the divertor tokamak plasma and present here preliminary results for some Balmer spectral lines of deuterium. For electron broadening estimation we consider the approximation 3 as a basic one. However, it requires a substantial amount of computation and therefore other approximations (such as 1 and 2) may be helpful. All results presented in this report are obtained for plasma temperature $T_e = T_a = 1$ eV.

In Fig. 1 we show the profile of the first Balmer line D_α calculated with using our approximation 3. The calculation is made for electron density $2.51 \cdot 10^{15}$ cm^{-3} (Fig. 1a) and $1.58 \cdot 10^{15}$ cm^{-3} (Fig. 1b), magnetic field $B = 6.2$ T and angle between directions of the magnetic field and observation $\widetilde{\vartheta} = 45^o$. This line splits into 36 Stark–Zeeman components which form three groups showing three peaks in the line profile with explicit asymmetry. The asymmetry appears only in the case of the use of the approximation 3 and can be explained by the different electron broadening of symmetrical components. Although the splitting structure is symmetrical, electron broadening of symmetrical components are different and, moreover, depends on the angle $\widetilde{\vartheta}$.

Figures 2 and 3 present the electron density dependence of the line width for the 6th deuterium Balmer member $\bar{n} = 8$ to $n = 2$. The width is defined in a usual manner as the distance between two points on the line profile, intensity of which is half of the maximal one. In Fig. 2 we compare the approximations 1, 2 and 3 without magnetic field ($B = 0$). We show here also the fitting curve (WG) from [14]

$$\Delta\lambda(Angstroms) = 2.5 \cdot 10^{-13}(0.229 N_e^{2/3} + 7.644 \cdot 10^{-7} N_e). \qquad (20)$$

Our approximations show similar behavior with (20) but lie lower than (20).

In Fig. 3 we compare our calculations obtained with the approximation 3 for three cases: a) $B = 0$, b) $B = 6$ T and direction of observation is normal to the magnetic field and c) $B = 6$ T and observation is along the magnetic field. Magnetic field gives rise to some increase of the width for electron densities $N_e < 2 \cdot 10^{15}$ 1/cm^3. If $N_e > 2 \cdot 10^{15}$ 1/cm^3 we have different dependencies for b) and c) cases. In b) case the width remains greater than

that in a) case while the width in c) case becomes less than the width without magnetic field.

In Figs. 4–12 we present the profiles for the 8–2 Balmer line for different electron densities without (Figs. 4–6) and with (Figs. 7–12) magnetic field $B = 6$ T. Profiles in Figs. 7–9 correspond to perpendicular directions of magnetic field and observation, while in Figs. 10–12 these directions are parallel. The profiles are normalized to $\int I_\lambda d\lambda = 1$, so the intensity is in inverse Angstroms. In Figs. 4, 7, 10 the profiles are presented for electron densities 10^{14}, $1.58 \cdot 10^{14}$ and $2.51 \cdot 10^{14}$ cm^{-3}; in Figs. 5, 8, 11 – $3.98 \cdot 10^{14}$, $6.31 \cdot 10^{14}$ and 10^{15} cm^{-3}; in Figs. 6, 9, 12 – $1.58 \cdot 10^{15}$, $2.51 \cdot 10^{15}$ and $3.98 \cdot 10^{15}$ cm^{-3}. Profiles without magnetic field have central dips usual for even members of the Balmer series. However strong magnetic field gives rise to appearance of central peaks because of complete change of the splitting structure. If one shall take into account ion-dynamical effects, these dips and peaks could partially be smoothed.

It should be noted that the 8–2 line can be considered as isolated for electron densities lower than 10^{16} cm^{-3}. For higher densities the line overlapping will be important.

References

[1] X. Bonin et al, Modelling of optically thick plasmas in Alcator C-Mod. 40^{th} APS Annual Meeting of the Division of Plasma Physics, New Orleans, November 1998.

[2] H. R. Griem, *Spectral Line Broadening by Plasmas*. Academic Press, New York (1974).

[3] M. Born, *Lectures on Atom Mechanics*, v. 1. ONTI, Kharkov (1934).

[4] Yu. N. Demkov, B. S. Monozon and V. N. Ostrovsky, Energy levels of the hydrogen atom in crossed electric and magnetic field. Zh. Eksp. Teor. Fiz. 57(4), 1431 (1969).

[5] D. A. Varshalovich, A. N. Moskalev and V. K. Khersonsky, *Quantum Theory of Angular Momentum*, Nauka, Leningrad (1975).

[6] H. A. Bethe and E. E. Salpeter, *Quantum Mechanics of One- and Two-Electron Atoms*, Springer-Verlag, Berlin (1960).

[7] A. F. Nikiforov and V. B. Uvarov, *Special Functions of Mathematical Physics*, Birkhauser, Basel (1988).

[8] V. S. Lisitza, Stark broadening of hydrogenic lines in plasma. Usp. Fiz. Nauk 122(3), 449 (1977)

[9] L. A. Vainshtein, I. I. Sobelman and E. A. Yukov. *Excitation of Atoms and Spectral Line Broadening*, Nauka, Moscow (1979).

[10] A. F. Nikiforov, V. G. Novikov and A. D. Solomyannaya, Self-consistent hydrogeniclike average atom model for matter with given temperature and density. Teplofiz. Vys. Temp. (High Temperature), 34(2), 220 (1996).

[11] B. Kivel, S. Bloom, H. Margenau, Phys. Rev. 98, 495 (1949).

[12] M. J. Seaton, Atomic data for opacity calculations: XIII. Line profiles for transitions in hydrogenic ions. J. Phys. B: At. Mol. Opt. Phys. 23(19), 3255 (1990).

[13] J. W. B. Hughes, Stark states and $O(4)$ symmetry of hydrogenic atoms. Proc. Phys. Soc. 91, 810 (1967).

[14] B.L.Welch, H.R.Griem, J.L.Weaver, J.U.Brill, J.Terry, B.Lipschultz, D.Lumma, G.McCracken, S.Ferri, A.Calisti, R.Stamm, B.Talin, R.W.Lee, Profiles of high principal quantum number Balmer and Paschen lines from Alcator C-Mod tokamak plasmas.

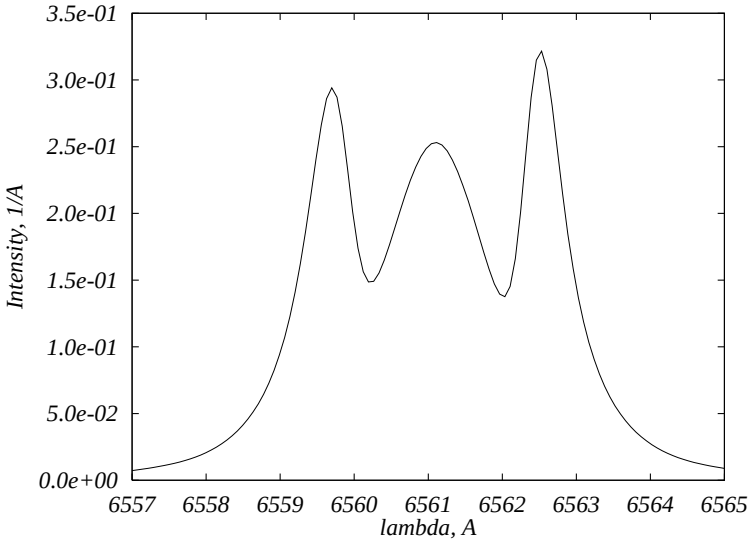
3.5e-01
3.0e-01
2.5e-01
2.0e-01
1.5e-01
1.0e-01
5.0e-02
0.0e+00
Intensity, 1/A
6557
6558
6559
6560
6561
6562
6563
6564
6565
lambda, A

a)

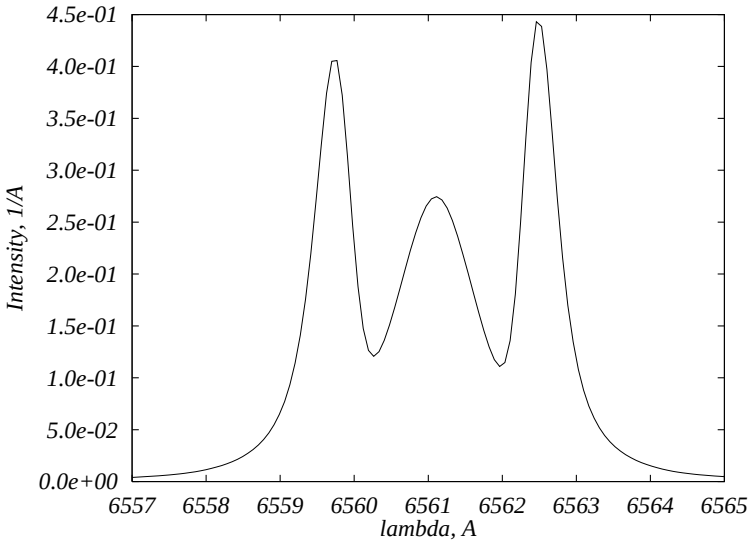
4.5e-01
4.0e-01
3.5e-01
3.0e-01
2.5e-01
2.0e-01
1.5e-01
1.0e-01
5.0e-02
0.0e+00
Intensity, 1/A
6557
6558
6559
6560
6561
6562
6563
6564
6565
lambda, A

b)

Figure 1.

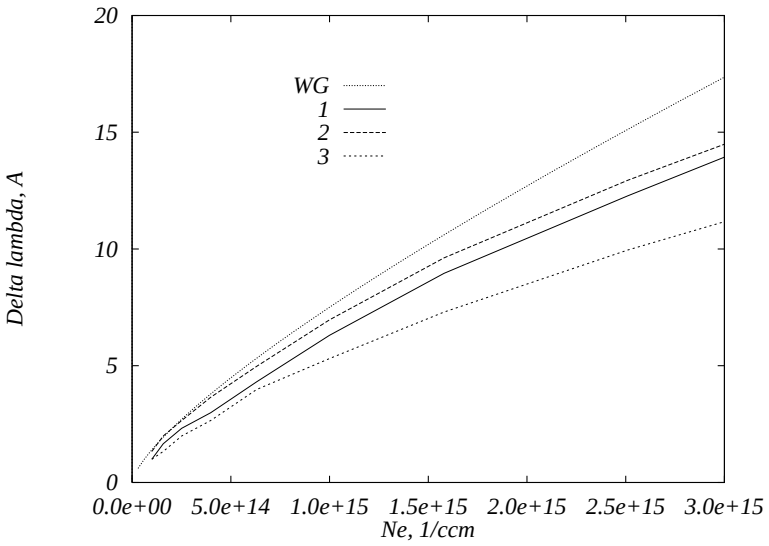

Figure 2.

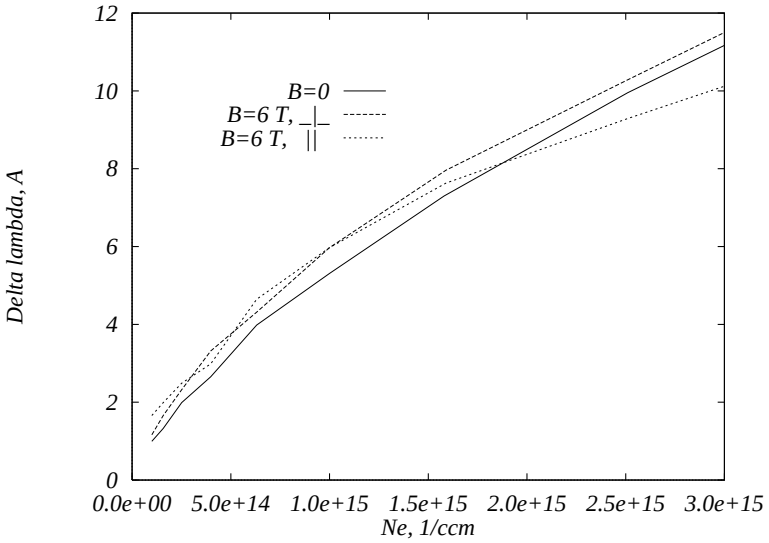

Figure 3.

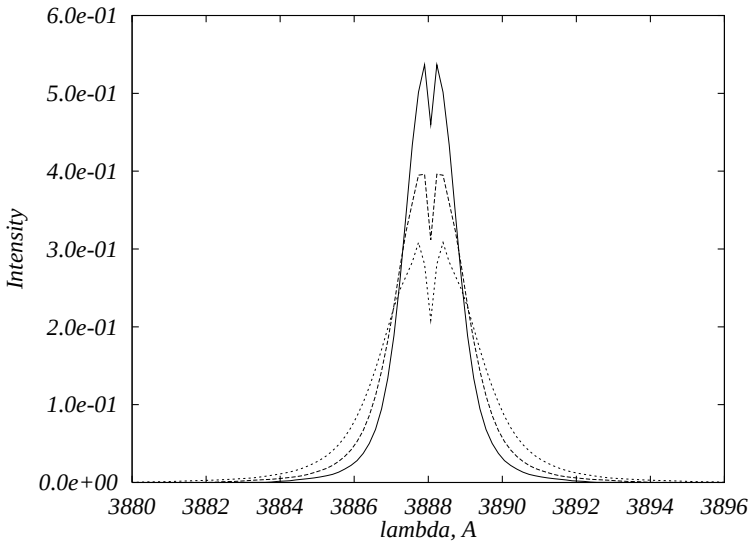

Figure 4.

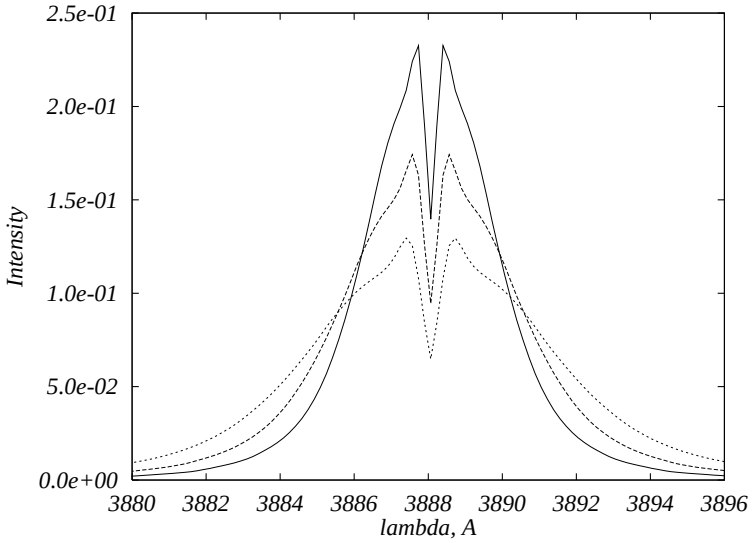

Figure 5.

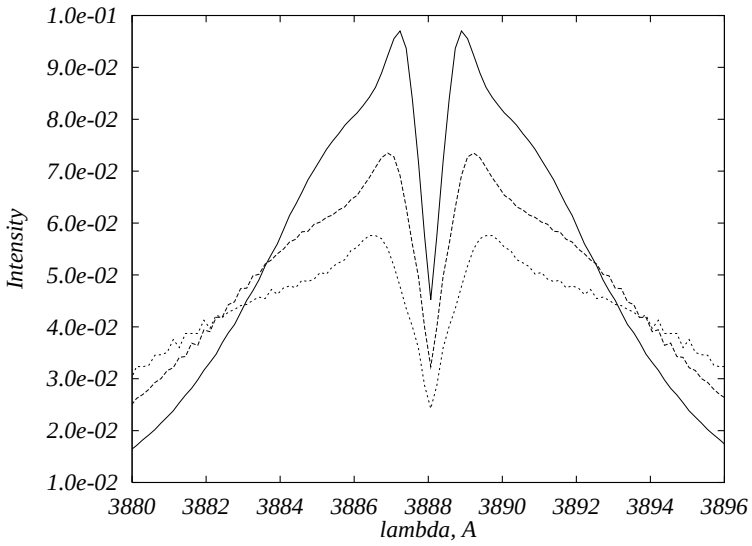

Figure 6.

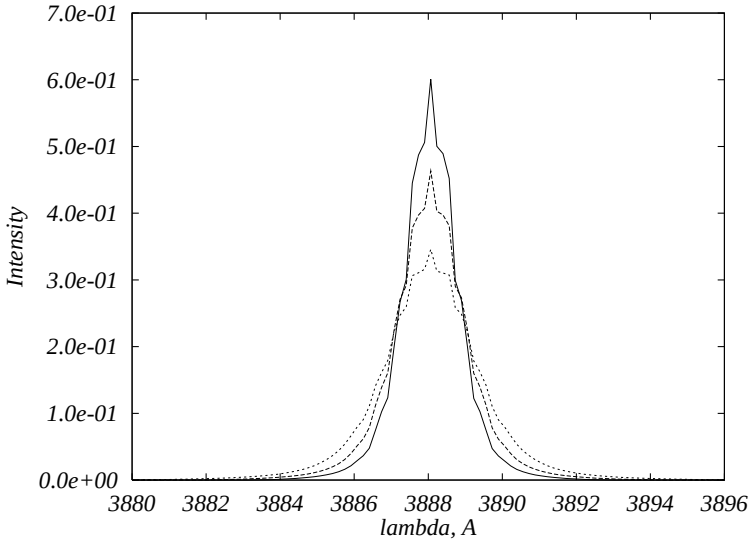

Figure 7.

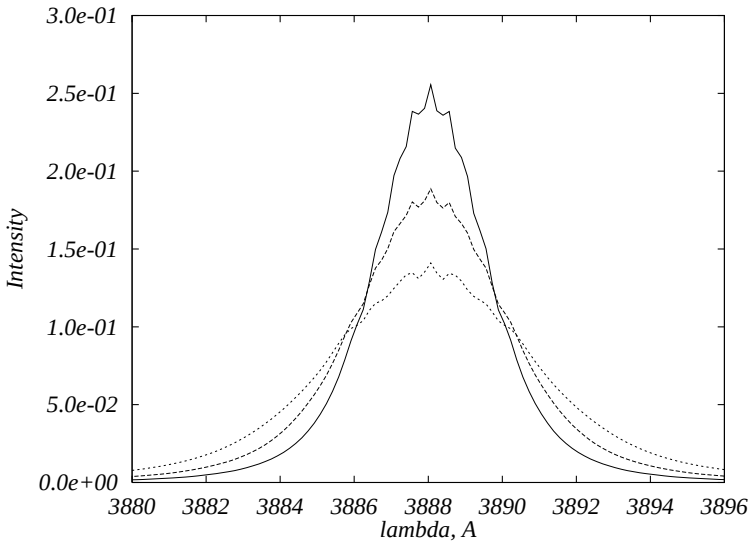

Figure 8.

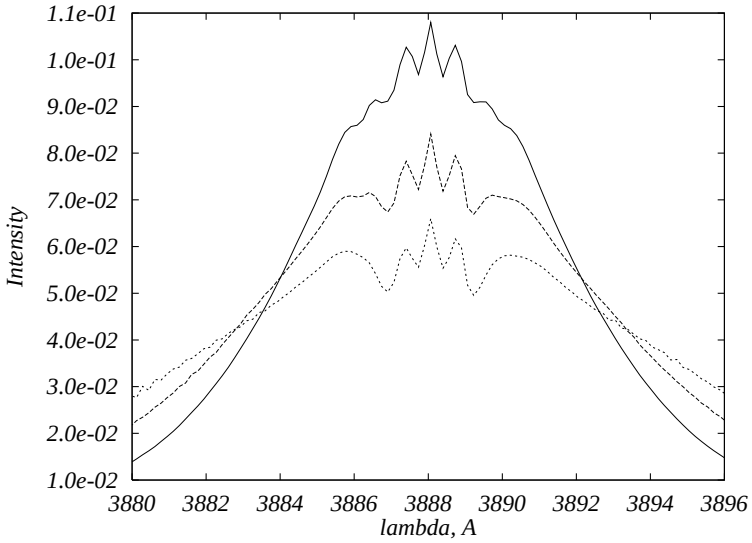

Figure 9.

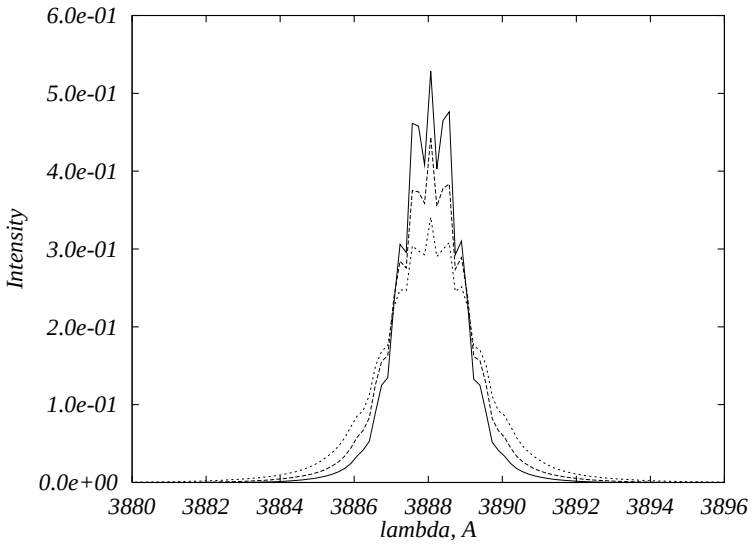

Figure 10.

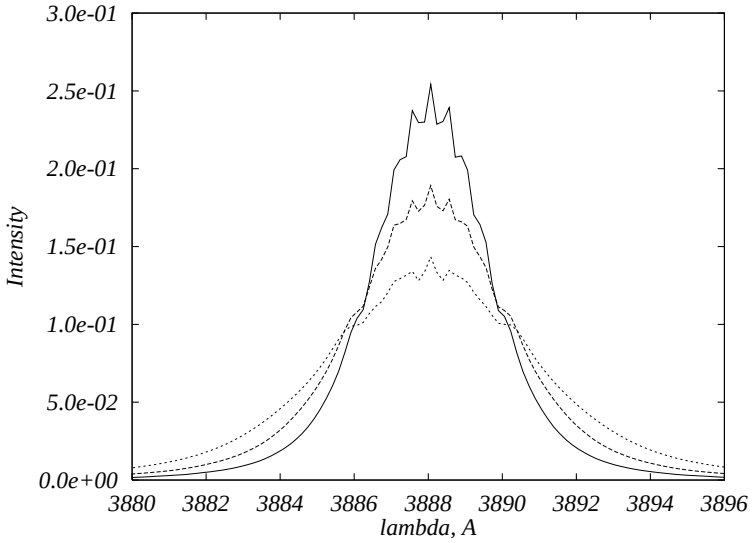

Figure 11.

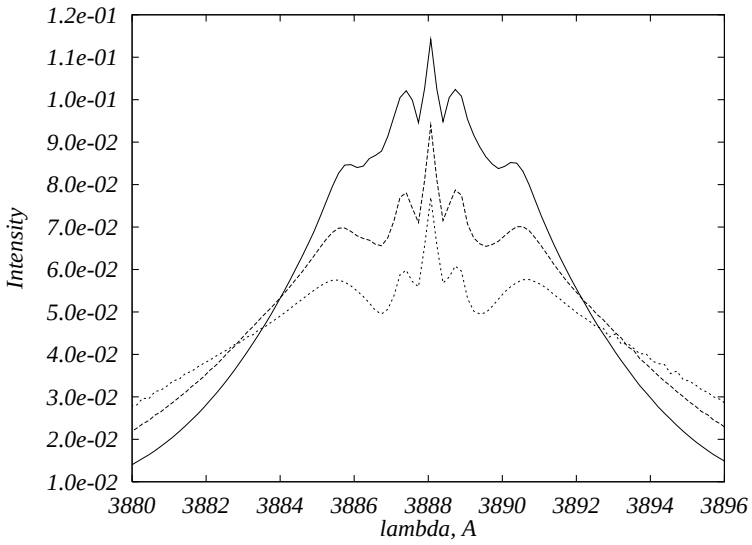
1.2e-01
1.1e-01
1.0e-01
9.0e-02
8.0e-02
7.0e-02
6.0e-02
5.0e-02
4.0e-02
3.0e-02
2.0e-02
1.0e-02
Intensity
3880
3882
3884
3886
3888
3890
3892
3894
3896
lambda, A

Figure 12.